DOI 10.1007/s11237-016-9477-3
Theoretical and Experimental Chemistry, Vol. 52, No. 4, September, 2016 (Russian Original Vol. 52, No. 4, July-August, 2016)

STRUCTURAL PROPERTIES OF SILICON CARBIDE NANO STRUCTURES GROWN ON QUARTZ SUBSTRATE USING CVD METHOD

A. Mahmoodi, M. Ghoranneviss, and Kh. Mehrani

UDC 544.2, 546.03

Silicon carbide (SiC) nanostructures were obtained by the chemical deposition of hexamethyldisiloxane ($C_6H_{18}OSi_2$) from the vapor phase onto quartz with a supported cobalt catalyst. A study was carried out on the structural and optical properties of the SiC nanostructures obtained at 650, 700, 750, and 800 °C using scanning electron microscopy, XRD, and electron spectroscopy. All the films were found to have crystalline structure. The optical transmittance in the visible region increases with increasing synthesis temperature.

Key words: *silicon carbide (SiC), nanostructures, nanomaterial.*

Considerable progress has been made in the past few decades on understanding the relationship between the processing of thin films, their microstructure on the nanometer level, properties, and nanodimensional structural characteristics [1-4]. Metal nanoparticles have been studied in light of their possible use in many applications [5]. Materials made with silicon carbide (SiC) hold interest due to their high heat resistance, good thermal conductivity, and hardness as well as their electrical properties. SiC is a material with a wide band gap. Such properties make SiC a promising material for high-output and high-temperature electronics. Micro-sized particles and whiskers of SiC are commonly used as reinforcement materials in the production of ceramics, metals, and alloys for various tribological applications and use in construction. The capacity of silicon carbide to function under extreme conditions may lead to considerable improvement of various functional materials [6-8].

The properties of SiC are directly related to its structure, which consists of alternating silicon and carbon layers [9]. The strong covalent bonds between the silicon and carbon atoms account for the high-frequency vibrations of its crystal lattice [10], generation of high-energy optical phonons (100-120 meV), which lead to a high rate of particle migration ($2 \cdot 10^7$ cm/s), and high thermal conductivity (490 W/(m·K)). The changes in the optical properties of SiC materials such as the index of refraction, absorption coefficient, and dielectric constant due to temperature variations are detected by changes in macroscopic optical properties such as reflectance [11]. In comparison with bulk and microdimensional silicon carbide, nanostructural silicon carbide has distinctive mechanical, electrical, and optical properties [12-15]. The yield strength of nanosized SiC is more than 50 GPa, which is substantially higher than for bulk silicon carbide [16]. SiC nanostructures are obtained by the reaction of carbon nanotubes either with silicon monoxide or with silicon and iodine vapors [17] in vapor–liquid–solid [18] or vapor–solid systems [19] by means of laser ablation [20] or chemical vapor deposition (CVD) [21].

In comparison with other CVD techniques, hot filament CVD (HFCVD) has a number of advantages such as the possibility of the deposition of thick layers on large areas and the coating of various types of substrate surfaces [22]; this technique is also easy to carry out. In the present work, we studied the growth of nanostructures of crystalline silicon carbide

Plasma Physics Research Center, Science and Research Branch, Islamic Azad University, P. O. Box 14665-678, Tehran, Iran. E-mail: na.mahmoodi@gmail.com. Translated from Teoreticheskaya i Éksperimental'naya Khimiya, Vol. 52, No. 4, pp. 256-261, July-August, 2016. Original article submitted May 10, 2016; revision submitted July 5, 2016.

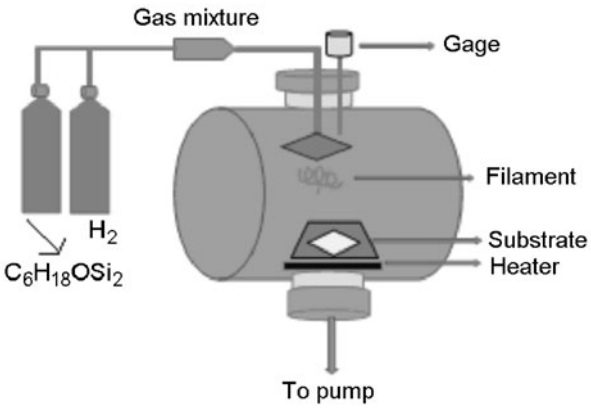

Fig. 1. Scheme of the system for synthesis of silicon carbide nanostructures.

from hexamethyldisiloxane (HMDSO, $O[Si(CH_3)_3]_2$ [23]) by the HFCVD method on a quartz substrate at various temperatures. Analysis of the resultant materials by scanning electron microscopy and XRD shows that the nanostructures have rhombohedral crystalline silicon carbide structure.

EXPERIMENTAL

We took 1×1-cm^2 quartz plates as the substrate. The plates were ultrasonically cleaned for 10 min in acetone and then ethanol baths and rinsed with distilled water. A cobalt target with 10-nm diameter was used as the cathode and was deposited onto the quartz substrate as the catalyst by plasma-enhanced chemical vapor deposition (PECVD). The PECVD reactor was constructed from a flat glass tube. The pressure in the reactor was maintained at pressure not above $3 \cdot 10^{-2}$ Torr. Voltage up to 1 kV was used to maintain the desired voltage on the electrodes. Argon was introduced at a rate of 120 mL/min into the chamber in order to maintain a pressure of $5 \cdot 10^{-1}$ Torr for 30 min during the deposition of cobalt onto the quartz plates. The deposition was carried out at low direct current of 120 mA in order to maintain glow discharge between the anode and cathode.

The synthesis of the silicon carbide nanostructures was carried out in a hot filament CVD system schematically represented in Fig. 1. The quartz substrate was placed onto a holder in the reaction chamber at the center of the furnace. The chamber was evacuated to 10^{-5} Torr taken as the base pressure to prevent oxidation of the metal upon heating to 500 °C for 10 min at 10 mm Hg. Hydrogen (H_2) was introduced in the reaction chamber at a flow rate of 100 mL/min in order to etch the substrate and activate the catalyst. During this operation, the temperature of the filament serving as the cathode was raised to 2000 °C. The process was carried out at 12 Torr over 10 min at different temperatures. A mixture of HMDSO and the hydrogen gas carrier was introduced into the reaction chamber through a bubbler in order to grow silicon carbide films at 650, 700, 750, and 800 °C. The synthesis was carried out at 2000 °C at low partial pressure of the precursor (12 mbar) using hydrogen at the gas carrier [24-27]. The morphology of the resultant silicon carbide nanostructures was studied with a Hitachi S4160 field emission scanning electron microscopy and the crystallinity of the nanostructures was analyzed by XRD on a STADI MP diffractometer (manufactured in Germany) using $K_{\alpha 1}$ radiation from a copper anode (λ = 1.5405 Å) with a tungsten filament at 40 kV and 30 mA as the electron source. The optical properties of the nanostructures were studied at room temperature using a Varian CARY 500 SCAN spectrophotometer in the UV-visible region.

RESULTS AND DISCUSSION

The X-ray diffraction (XRD) revealed the phase composition of the analyzed films and showed whether they were crystalline or polycrystalline. The XRD spectra of the samples prepared at 650, 700, 750, and 800 °C are given in Fig. 2a-d and

TABLE 1. Dependence of the Length and Diameter of the SiC Nanostructures on the Synthesis Temperature

Temperature, °C	Diameter, nm	Length, nm
650	225	220
700	255	433
750	438	874
800	432	2292

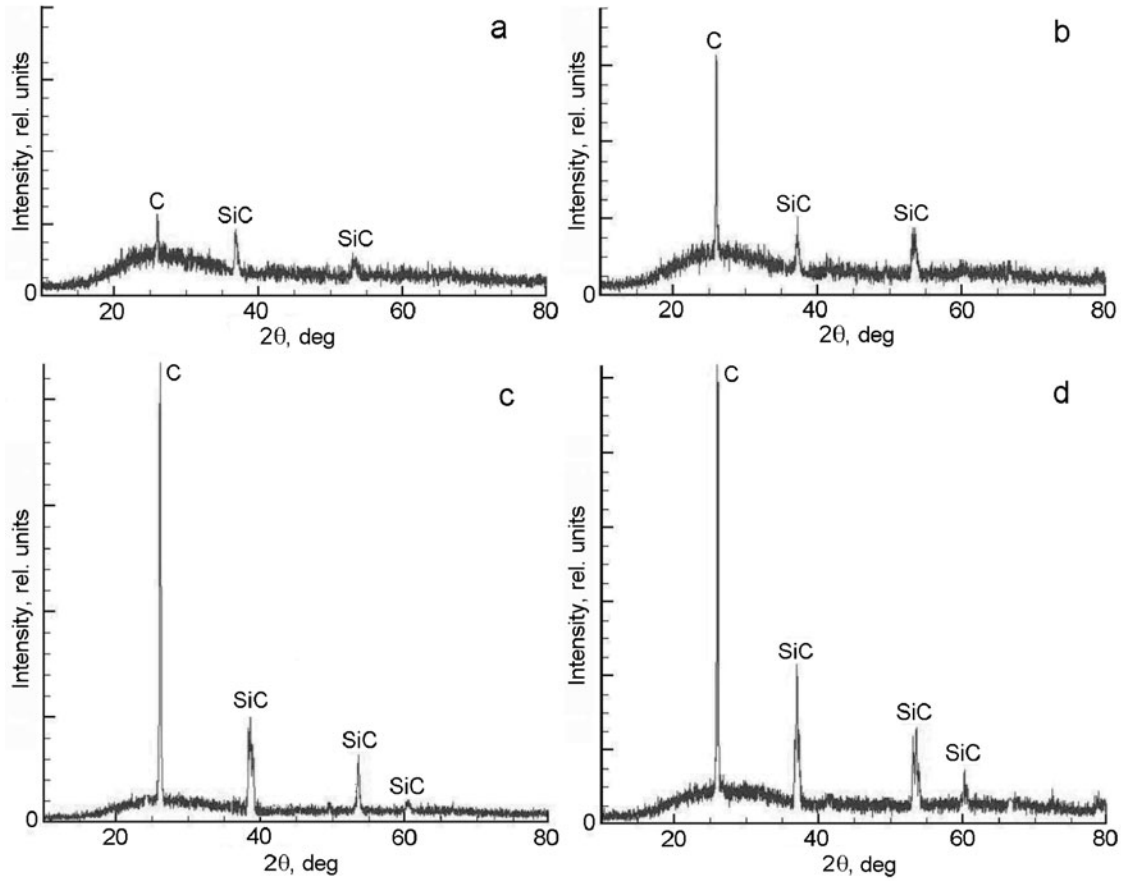

Fig. 2. XRD spectra of samples synthesized at 650 (a), 700 (b), 750 (c), and 800 °C (d).

show that all the samples contain diffraction peaks for graphite (C, hexagonal) and silicon carbide. The major peaks are observed at 26.04°, 37.093°, 53.446°, and 60.46°, where the peak at 26.04° corresponds to graphite and the others correspond to silicon carbide. The peak at 60.46° for samples obtained at 650 and 700 °C is weak and may be ignored. On the other hand, a significant peak at 60.46° corresponding to SiC appears for samples prepared with substrate temperature above 700 °C. These data indicate that increasing temperature leads to increasing peak intensity as the result of increased crystallinity of the samples.

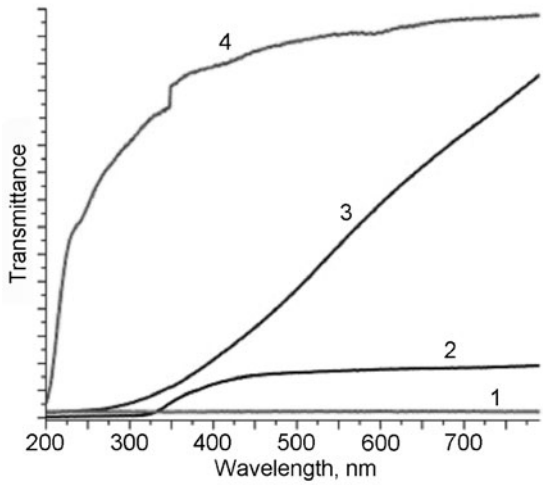

Fig. 3. Transmittance spectra of SiC nanostructures obtained on a quartz substrate at 650 (a), 700 (b), 750 (c), and 800 °C (d).

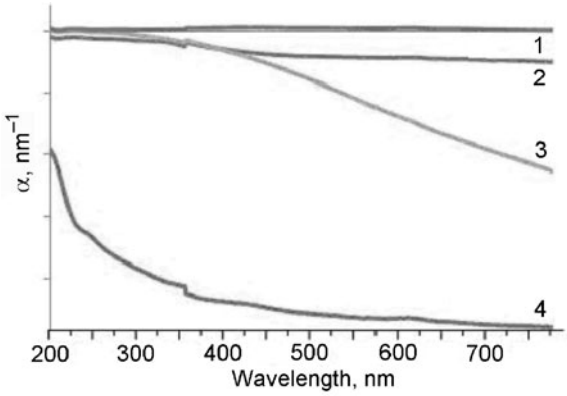

Fig. 4. Absorption spectra of SiC nanostructures obtained on a quartz substrate at 650 (a), 700 (b), 750 (c), and 800 °C (d).

The XRD data also indicate that the SiC nanostructures have a rhombohedral crystal lattice. The silicon carbide nanostructures obtained at 800 °C are the most crystalline.

The axes and angles in the rhombohedral system are analogous to the hexagonal system. The primitive unit cell is a rhombohedron with parameters $a = b = c$ and $\alpha = \beta = \gamma \neq 90°$. Table 1 gives the dimensions of the SiC nanocrystals depending on their synthesis temperature. These data suggest that increasing the temperature of deposition leads to a decrease in the size of the silicon carbide crystal. This behavior may be attributed to the creation of several nucleation sites on the surface, which leads to the formation of smaller crystals.

Figure 3 gives transmittance spectra of all the prepared silicon carbide nanostructures deposited onto quartz substrates at different temperatures. Figure 4 gives the corresponding absorption spectra of the SiC nanostructures. The data in Fig. 3 indicate that transmittance is characteristic for all the samples subjected to heat treatment. An increase in the optical transmission coefficient is clearly seen upon increasing the substrate temperature during the synthesis process up to 800 °C.

The SEM images of the resultant films are given in Fig. 5, which clearly shows the morphology of their surface with many fine crystals consisting of silicon carbide nanostructures, whose size increases with increasing synthesis temperature.

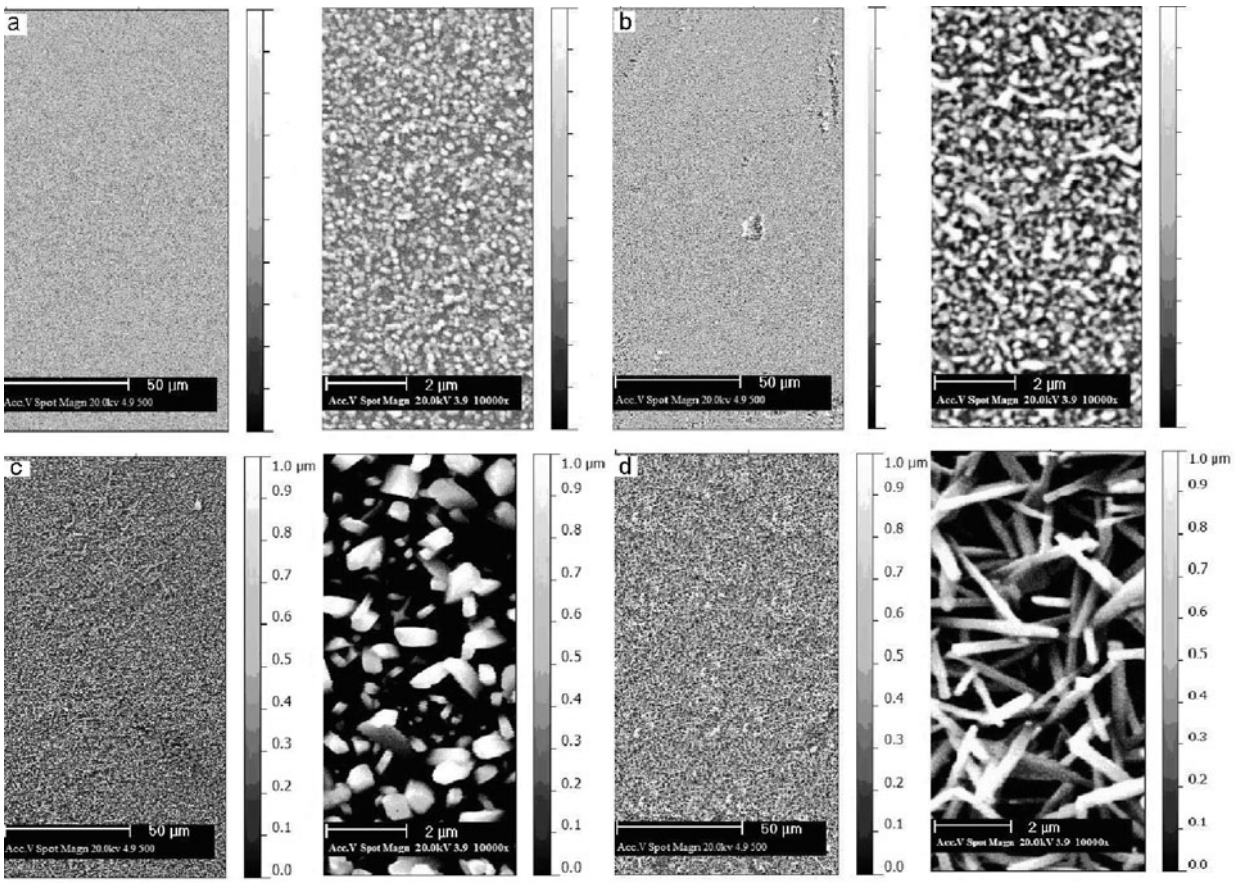

Fig. 5. SEM images of SiC nanostructures obtained at 650 (a), 700 (b), 750 (c), and 800 °C (d).

These crystals are formed at temperatures from 650 to 800 °C. All these films have homogeneous distribution of the prepared SiC over the entire surface on a scale of 50 μm.

The images in Fig. 5 for scale 2 μm indicate that the length of the nanostructures increases with increasing synthesis temperature from 650 to 700 °C, while their diameter remains virtually unchanged. The density of the nanorod distribution depends on the synthesis temperature. The lengths and diameters were measured for a series of nanostructures in the presented SEM images selected at random. The relationship found between the nanostructure dimensions and the preparation temperature is given in Table 1. Microcrystals and rodlike structures were observed on the surfaces at 750 and 800 °C. In addition, the length of the nanostructures synthesized at 800 °C was much greater than for the nanostructures synthesized below 750 °C, apparently due to an increase in the rate of entry of silicon vapor at higher temperature.

Thus, SiC nanostructures were synthesized from $C_6H_{18}OSi_2$ at different temperatures and pressure 12 mm Hg. The synthesis temperature was varied from 650 to 800 °C and nanostructure growth was seen at all the temperatures. The XRD data indicate that the resultant silicon carbide has rhombohedral structure and the crystallinity of the silicon carbide increases with increasing temperature of the substrate. The transmission coefficient of the silicon carbide nanostructures increases with increasing temperature of their synthesis, leading to a decrease in optical absorption. Nanostructures with length from 2 to 20 μm were obtained depending on the synthesis temperature. Analysis of the SEM data shows that the length of the nanostructures increases with increasing temperature. In comparison with other reported methods for the synthesis of nanocrystalline SiC, the major advantage of our method is relatively low temperature for the synthesis of this material.

REFERENCES

1. S. Talu, S. Stach, T. Ghodselahi, et al., *J. Phys. Chem. B*, **119**, 5662-5670 (2015).
2. S. Talu, S. Stach, S. Solaymani, et al., *J. Electroanal. Chem.*, **749**, 31-41 (2015).
3. S. Talu, Z. Markovics, S. Stach, et al., *Appl. Surface Sci.*, **289**, 97-106 (2014).
4. S. Stach, Z. Garczyk, S. Talu, et al., *J. Phys. Chem. C*, **119**, 17887-17898 (2015).
5. A. Armana, T. Ghodselahib, S. Solaymani, et al., *Proc. Met. Phys. Chem. Surfaces*, **51**, No. 4, 575-578 (2015).
6. V. A. Dmitriev, *Status of SiC Technology: Bulk and Epitaxial Growth*, International Technology Research Institute, Technology Transfer (TTEC) Division (2000) (TTEC Panel Report on High-Temperature Electronics in Europe, Chap. 2).
7. D. Z. Wang, H. X. Peng, J. Liu, et al., *Wear*, **184**, 187-192 (1995).
8. I. Garcia, J. Fransaer, and J. P. Celis, *Surface Coat. Technol.*, **148**, 171 (2001).
9. P. Colomban, *Silicon Carbide – Materials, Processing, and Applications in Electronic Devices*, M. Mukherjee (ed.), InTech (2011).
10. H. Matsunami, *Jpn. J. Appl. Phys.*, **43**, 6835-6847 (2004).
11. J. Mazumder and A. Kar, *Theory and Applications of Laser Chemical Vapor Deposition*, Plenum Press, New York (1995).
12. E. W. Wong, P. E. Sheehan, and C. M. Lieber, *Science*, **277**, 1971-1975 (1997).
13. X. D. Han, Y. F. Zhang, K. Zheng, et al., *Nano Lett.*, **7**, 452 (2007).
14. H. W. Shim, J. D. Kuppers, and H. C. Huang, *Nanotechnology*, 025704 (2009).
15. S. Z. Deng, Z. B. Li, W. L. Wang, et al., *Appl. Phys. Lett.*, **89**, 023118 (2006).
16. Z. W. Pan, H. L. Lai, F. C. K. Au, et al., *Adv. Mater.*, **12**, 1186-1190 (2000).
17. G. W. Meng, L. D. Zhang, C. M. Mo, et al., *J. Mater. Res.*, **13**, 2533-2538 (1998).
18. S. Z. Deng, Z. S. Wu, J. Zhou, et al., *Chem. Phys. Lett.*, **256**, 511 (2002).
19. J. J. Niu, J. N. Wang, and Q. F. Xu, *Langmuir*, 6918 (2008).
20. W. S. Shi, Y. F. Zheng, H. Y. Peng, et al., *J. Am. Chem. Soc.*, **83**, 3228 (2000).
21. J. Wei, K. Z. Li, H. J. Li, et al., *Mater. Chem. Res.*, **95**, 140 (2006).
22. S. A. Rakha, Z. Xintai, D. Zhu, and Y. Guojun, *Curr. Appl. Phys.*, **10**, 171 (2010).
23. J. Pfeifer, *Encyclopedia of Reagents for Organic Synthesis*, L. Paquette (ed.), J. Wiley & Sons, New York (2004), doi: 10.1002/047084289.
24. H. Lin, J. A. Gerbec, M. Sushkhid, and E. W. McFarland, *Nanotechnology*, **19**, 325601 (2008).
25. V. Kopustinskas, S. Meskinis, V. Grigaliunas, et al., *Surface Coat. Technol.*, **151**, 180-183 (2002).
26. V. Kopustinskas, S. Meskinis, S. Tamulevičius, et al., *Surface Coat. Technol.*, **200**, 6240-6244 (2006).
27. F. Roccaforte, F. Giannazzo, F. Iucolano, et al., *Appl. Surface Sci.*, **256**, 5727-5735 (2010).